COMPARISON OF FIBRE FROM MAIZE STALK DOMAINS AND SUGAR CANE BAGASSE

Thulani Shabangu, Linda Z. Linganiso, Tshwafo E. Motaung
University of Unizulu Kwadlangezwa, Department of Chemistry
Kwadlangezwa Campus
South Africa

Motloung V. Setumo
Nelson Mandela University, Department of Physics
Port Elizabeth, South Africa

Lehlohonolo F. Koao
University of The Free State, Department of Physics, Qwaqwa Campus
Phuthaditjhaba, South Africa

ABSTRACT

The aim of this study is to investigate properties of pulverised cellulosic material from parts of maize stalks and sugar cane bagasse (SCB). Both materials were foremost subjected to a cutting mill before boiling with water. The chemical compositions and mechanical properties of the maize stalk residues and sugar cane bagasse were performed using a TAPPI standard. Optical microscope, Fourier-transform infrared spectroscopy (FTIR), X-ray diffraction (XRD), thermogravimetric analysis (TGA) and Ultraviolet-visible spectroscopy (UV-Vis) were used to characterise the materials. Rind displays thinner and longer fibres, which are less unequal and almost quadrangular. In fact, it has a highest crystallinity trailed by nodes and sugar cane bagasse in sequence. Interestingly, thermal stability of SCB is dominating followed by rind and nodes.

INTRODUCTION

Biomass ranks third largest primary energy resource globally. The consumption of biomass energy ranges from 40% to 50% in developing countries due to high agricultural practices (Gramera and Whistler 1963, Song et al. 2004, Sun et al. 2014, Zhang et al. 2016). Corn stalk and sugar cane bagasse are lignocellulosic materials that are amongst the most abundant biomass among crop-based remnants. The materials consist mainly of three chemical components which

are cellulose, lignin and hemicellulose that are bonded together by intermolecular bridges and Van der Waals forces (Zhao et al. 2013, Sun et al. 2015, Ioannidou et al. 2009). Genetic and environmental factors influence the chemical compositions across different parts of their anatomy (Ye et al. 2008).

The annual world generation of sugarcane bagasse and leaves was ~279 million metric tons, in 2010 (Chandel et al. 2012). Sugarcane results contain 30% of bagasse, which is used to produce electricity for mill use. The bagasse, corn stalk and other lignocellulosic biomass can be directly converted into useful organic compounds, such as ethylene glycol, and 1,2-propylene glycol (Sun et al 2015). Most recent lignocellulosic biomass applications use cellulose, lignin, or hemicelluloses. Agricultural remnants like wheat straw and corn stalks are renewable biomass resources that can be used as a backup source for the production of bio-phenols because of their lignin content, for making particleboard and oil production (Wang and Sun 2002, Wang et al. 2009). Other lignocellulosic biomass applications are hydrogen production (Ren et al. 2008, Cheng and Liu 2011, Xing et al. 2011, Jiang et al. 2016), production of 5-hydroxymethylfurfural (Yan et al. 2014), ethanol production, cement production (Yang et al. 2011, Cheng and Liu 2011, Xu et al. 2015, Quesada et al. 1999, Song 2009, Jarabo et al. 2013) and papermaking (Pažitný et al. 2013). Sugarcane bagasse can produce electricity, enzymes, activated carbons, bio-hydrogen, ethanol, xylitol, organic acids and methane (Zeng et al. 2014, Kalderis et al. 2008, Martın et al. 2002, Chandel et al. 2012).

One of the latest common applications of lignocellulosic biomass is biofuels production due to its renewability, abundance and environmental friendliness (Li et al. 2016a). Besides protecting polysaccharides in the plant cell wall, lignin adsorbs onto a catalyst and hinders catalytic hydrogenesis. Depolymerisation of polysaccharides to simple sugars enables their effective conversion to ethanol, biofuels and other valuable products. Only few microorganisms are able to degrade lignin due to the complexity and variability of its structure. Thermo-chemical pre-treatment is required to remove or delocalize lignin before the biomass hydrolysis. The overall efficiency of biomass conversion highly depends on improvement of pre-treatment technologies, specifically the effectiveness of lignin modification. There is more research interest in pre-treatment technology, aiming to improve the degradability of lignocellulosic materials. The recent pre-treatment methods include acid, alkali, steam explosion and steam extrusion (Gigac et al. 2017, Stankovská et al. 2018, Pažitný et al. 2019a, Pažitný et al. 2019b), liquid hot water, sodium hydroxide treatment, ammonia fibre explosion and their combinative pre-treatments (Sun et al. 2015, Zeng et al. 2014, Gao et al. 2013). The increasing petrol price, greenhouse gas emissions, and the lignocellulosic biomass abundance motivated to the development of wood adhesives from a renewable substances. Lignin has been used as a replacement for phenol in phenolic resin synthesis (Wang et al. 2009). The conversion and modification of corn stalk into simple sugars without combustion (Song et al. 2009) include ozonation of lignin rich fractions (Singh et al. 2017), preparation activated carbons for air and wastewater purification (Li et al. 2016b, Cao et al. 2016). Preparation of adsorbents and their specific application in metal ions adsorption (Wang et al. 2016) involve evaluation and optimization of pre-treatment techniques for catalytic hydrogenolysis conversion of corn stalk into polyol (Sun et al. 2014).

According to experts' estimations, by 2030, 20% of transportation fuel and 25% of chemicals produced in the US will be from biomass (Wang et al. 2009). Lignocellulosic materials are abundant, renewable resources on the earth and could be a potential alternative for energy generation in the future (Pang et al. 2012, Song et al. 2015, Uzun and Sarioğlu 2009). When the thermo-chemical pre-treatment technology is perfected, second generation ethanol will be produced from sugarcane bagasse, which has been used for power generation (Zeng et al. 2014).

Physical pre-fractionation of botanical corn stalk fractions concentrates higher value components; reduces drying costs, and upgrades transportation and utilization efficiencies of a spacious, chemically diverse feedstock (Ye et al. 2008). Lignocellulosic chemical constituents have different applications. The quantification of cellulose, hemicelluloses, and lignin in all the selected corn stalk fractions can help with the identification of an appropriate fraction for a specific application. Therefore, this study quantifies and compares the concentrations of cellulose, hemicelluloses, and lignin in pre-treated corn pith, nodes, rind, and sugarcane bagasse.

MATERIAL AND METHODS

Materials

Corn stalks were collected from a local farmer in Empangeni area. Sugar cane bagasse was supplied by Tonga at Hullet Company Mills Walk, Felixton, Empangeni, 3875.

Pre-fractionation

Corn stalk was fractionated into nodes, rind, and pith using the electric saw. Rind, pith, nodes, and sugarcane bagasse (SCB) were each pulverized to a particle diameter of 0.25 mm using the cutting mill pulverisette 15. The powders were each boiled with distilled water for an hour. The process was repeated for four times. The samples were dried in the oven for 24 hours at 50°C.

Chemical composition

The SCB untreated and other untreated samples in this work were used to determine their respective chemical composition. The lignin, cellulose and hemicelluloses contents were determined according to the TAPPI Standards.

Characterization

The SEM and EDX measurements of the deposited thin films were performed on a Philips XL 30 FEG (at 10 kV) and DX4 detector (at 20 kV), respectively. The films were carbon-coated by using Edward's E306A coating system, prior to the analyses. FTIR spectroscopy analysis was carried out on a Bruker Tensor 27 FTIR spectrometer using a standard ATR cell; the catalysts were analysed as synthesised with no prior preparation required. The force was adjusted to 90 gauge for sufficient contact between the surfaces.

The catalysts were scanned over the mid-IR region (450-4000 cm^{-1}). The XRD characterization of all samples was performed on Powder X-Ray Diffraction spectroscopy (Bruker AXS Advance D8 diffractometer) with monochromatic Cu Kα (λ = 1.5406 Å) incident radiation at 40 kV and 40 mA at room temperature. The samples were scanned within the high angle 2θ range to get all characteristic diffractions of the materials at 0.5 scan speed and 0.01314 increments. Thermogravimetric analyses were performed using TGA analyser unit (Perkin Elmer), under flowing nitrogen atmosphere at flow rate of 20 mL·min^{-1}. Approximately 10-15 mg of a sample was heated from 25°C to 600°C at a heating rate of 10°C·min^{-1}. The sample weight loss and rate of weight loss were recorded continuously as functions of temperature. The analysis was only started when isothermal condition had been obtained. Optical absorption measurements of the nanoparticles were carried out using a Perkin-Elmer Lambda 1050 NIRUV-Visible spectrophotometer. The samples were placed in silica cuvettes (1 cm path length), using water as a reference solvent.

RESULTS AND DISCUSSION

Chemical composition

Tab. 1 displays the percentage contents of cellulose, lignin and hemicelluloses in SCB, nodes, pith and rind. The material was analysed after milling as shown in Fig. 1.

Tab. 1: Composition of used lignocelluloses.

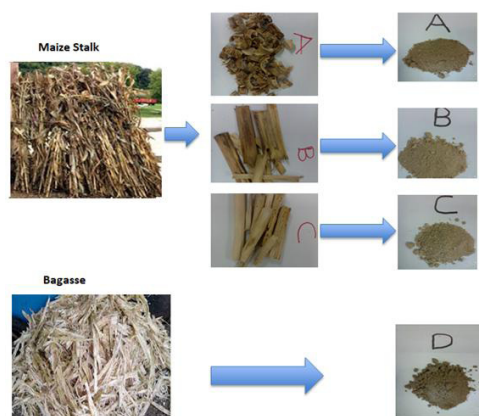| Component	Cellulose (%)	Lignin (%)	Hemicelluloses (%)
SCB	33	21	46
Nodes	35	16	49
Pith	34	14	52
Rind	36	17	47

Fig. 1: Images of three parts of maize stalk and sugarcane bagasse.

By the way it is clear from the images that all the powders are similarly dark in colour. Interestingly the chemical compositions remain independent. Hemicelluloses content dominates the rest components for all materials. This is not common in literature, but various reasons such as biodegradation stage, source of the material, harvesting period, storage and experimental uncertainties are possible validations for the observation (Song et al. 2009, Zabaniotou and Ioannidou 2008, Jiang et al. 2016). The rind is the richest in cellulose followed by nodes, while pith and nodes are richest in hemicelluloses.

Optical microscope (OM)

Fig. 2a, 2b, 2c, 2d show the microscope images of nodes, rind, pith and SCB sequentially. The irregularity in shape of the fibres in the images is evidently all over and it is accompanied by what looks like random dispersion of dark particles (see the arrows). Rind displays thinner and longer fibres, which are less irregular and almost rectangular. Nodes, pith and SCB display the dominance of shorter fibres, which are more irregular and amorphous in shape. There seems to be a remarkable resemblance between nodes and SCB. They both contain more of dark particles (where size is smaller than 50 μm) than of both rind and pith (size of particles is approximately 120 μm). Another similarity is the looser and smaller fibre bundles than rind and pith. There are whole lot of possible reasons for our observations in literature including the nature and the source of fibre. However, in this study the fibres clearly responded differently from the same preparation.
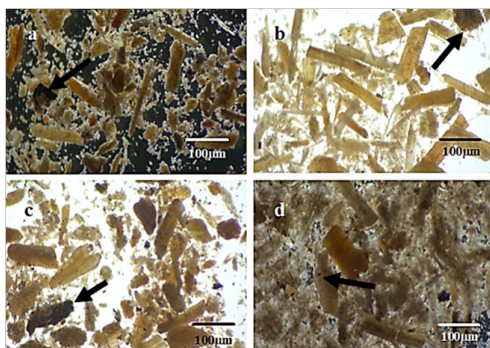
Fig. 2: Optical microscope images of a) Node, b) Rind, c) Pith and d) SCB.

Fourier transform infrared (FTIR) spectroscopy

Fig. 3 displays the FTIR spectra for bagasse, nodes, pith and rind. All spectra display the typical behaviour of natural fibres. The common absorption peaks for all four spectra appear around 3343 cm⁻¹, 1604 cm⁻¹, 1243 cm⁻¹, 1243 cm⁻¹, 1035 cm⁻¹, and 559 cm⁻¹. Those are normally attributed to O-H stretch, C=C (aromatic), O-H vibration from a phenolic group, O–H/C-O/C=C/C-C-O stretching, and C–C stretching, respectively (Ragan and Megonnell 2011, Xu and Wang 2015).
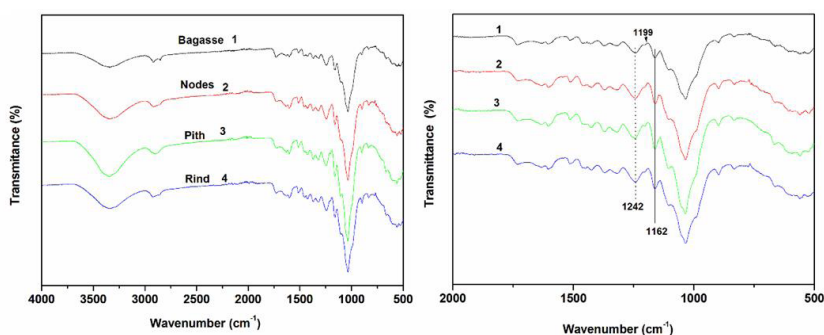

Fig. 3: FTIR spectra of SCB, nodes, pith and rind.

The O-H peak has the highest intensity for pith as compared to SCB, nodes and rind. This indicates the relatively highest O-H bond density for pith and the lowest for bagasse. Most functional groups indicated in above spectra are associated with lignin, cellulose and hemicelluloses (Quan et al. 2016, Nanda et al. 2013, Yang et al. 2007, Pažitný et al. 2011).

Thermogravimetric (TG) analysis

Fig. 4 represents the thermal stability and DTG curves of SCB, pith, nodes, and rind in nitrogen atmosphere. Thermograms of all samples display three-step degradations as confirmed by derivative TG curves (DTG). Temperatures of the thermal events are confirmed in Tab. 2. It is well known that a moisture removal, degradation of holocellulose and cellulose are normal order of increasing temperature for the peaks. The band of the lignin is negligible as it apparently degrades throughout the temperatures of the second and third peaks.
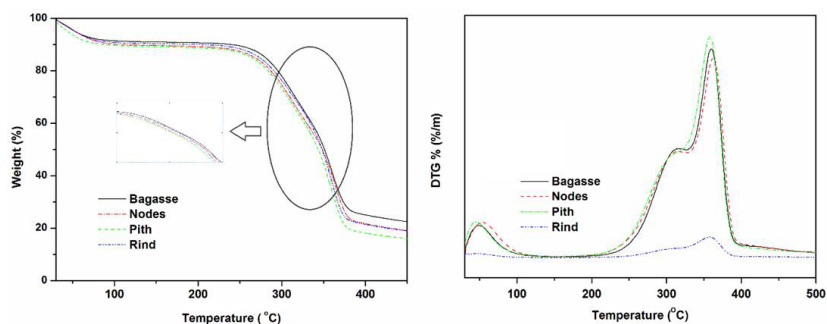
Fig. 4: Thermograms (TG, DTG) for sugarcane bagasse, nodes, pith and rind.

Thermal stability of SCB is dominating followed by rind and nodes consecutively. The trend is clearer around 400°C. The relatively higher yield for SCB after decomposition is attributed to lignin as seen in the composition analysis. There is nothing less than hemicelluloses which rendered the pith the least yield; whereas the cellulose is probably responsible for the yield of the rind and nodes (Quan et al. 2016, Poletto et al. 2010, Xiao et al. 2001).

Tab. 2: Peak temperatures for SCB, nodes, pith and rind.

Component	Number of peaks	Peak 1 (°C)	Peak 2 (°C)	Peak 3 (°C)
Bagasse	3	45.27	313.32	362.74
Nodes	3	49.18	310.83	362.74
Pith	3	30.34	314.03	358.83
Rind	3	48.47	312.25	359.54

X-ray diffraction (XRD) analysis

Fig. 5 displays the XRD bands for SCB, nodes, pith and rind. All samples display typical biomass diffractogram with amorphous and crystalline peaks around 15.50 and 220. A highest reflection is observed at around 21.50^0, which is normally attributed to arrangement of cellulose while the amorphous lignin and hemicelluloses could account for halo part across the peak. Crystallinity index (CI) was calculated using the peak height method from which CI = [(I_{002}- Iam) /I_{002}]*100. CI is crystallinity index, I_{002} is the intensity of the crystalline peak, and Iam is the intensity the amorphous peak. Tab. 3 displays crystalline indices, amorphous and crystalline peak intensities of SCB, nodes, pith and rind. According to CI calculations, rind is mostly crystalline, followed by nodes, SCB, and pith, respectively. Higher crystallinity indicates the relatively higher cellulose II content in rind and nodes, respectively. Pith appears to be the most amorphous fraction compared to other lignocelluloses studied in this work, which suggests higher content of amorphous hemicelluloses, cellulose I or lignin (Nanda et al. 2013, Corrales et al. 2012, Focher et al. 2001, Xiao et al. 2001, Singh et al. 2017). This somehow explains its low thermal stability since the lignin is known for accelerating thermal degradation of natural fibres (Quan et al. 2016, Singh et al. 2017, Kline et al. 2010, Scardi and Leoni 2001, Corrales et al. 2012).
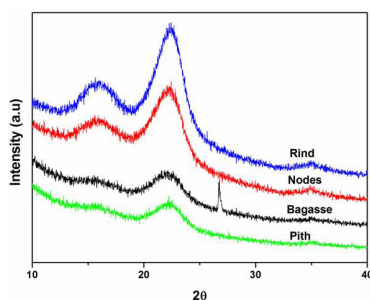
Fig. 5: XRD diffractograms for SCB, nodes, pith and rind.

Tab. 3: The crystalline, amorphous peak intensities and crystalline indices for SCB, nodes, pith and rind.

Sample	I_{002} Intensity	I_{am}	CI
Sugarcane bagasse	862.44	798.43	7.40%
Nodes	1676.03	1313.87	21.61%
Pith	724.31	717.58	0.93%
Rind	2151.54	1455.36	32.36%

UV-Vis spectroscopic analysis

Fig. 6 represents the UV-Vis spectra for SCB, nodes, pith and rind. Tab. 4 summarises the maximum peak wavelengths and absorbance for all samples.
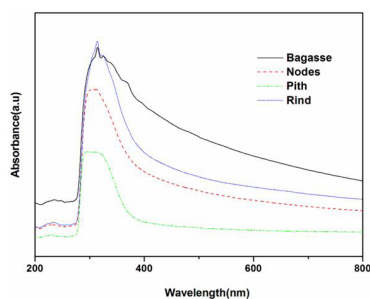

Fig. 6: UV-Vis spectra for SCB, nodes, pith and rind.

Form Fig. 6 and Tab. 4, it can be seen that samples absorb in the visible region. Each band displays a single dominant peak where maximum is at 314, 304, 296, and 314 nm for SCB, nodes, pith, and rind respectively.

Tab. 4: Maximum UV-Vis peak wavelength and absorbance for SCB, nodes, pith and rind.

Component	Peak wavelength (nm)	Absorbance (μ.S)
Sugarcane bagasse	314.08	3.61
Nodes	304.05	2.84
Pith	296.12	1.68
Rind	314.08	3.70

The peak around 290 nm is associated with the C=O π-electron excitations. The shift of bands to higher wavelength for SCB, nodes and rind could be due to the increased conjugation of C=O bonds. The absorption of SCB and rind at a wider wavelength range is also attributed to increased conjugation. The highest peak for rind indicates the highest absorption coefficient followed by SCB, nodes and pith respectively.

CONCLUSIONS

The spectral data collected in this study indicate that sugarcane bagasse, maize nodes, pith and rind do not have the same content of hemicelluloses, cellulose and lignin. XRD and TG analysis detected notable variations in morphology and thermal properties between SCB, node, pith and rind. FTIR and UV-VIS method detected remarkable differences in functional group distribution and chromophores conjugation between investigated samples. SCB and nodes could be potential feedstock candidates for lignin based biomass applications, while pith could be appropriate for hemicelluloses, and rind for cellulose-based applications. Selective use of corn stalk fractions for relevant applications may help cut the industrial biomass waste. The quantification and comparison of hemicelluloses, cellulose and lignin from SCB, nodes, pith and rind is a potential advancement from this work and could help quantify the amount of industrial biomass waste for relevant applications. The knowledge from this study can contribute to the further understanding of the differences in physical properties of cornstalk fractions, effective use of biomass residues and industrial biomass waste reduction.

ACKNOWLEDGEMENTS

REFERENCES

1. Cao, Y., Wang, K., Wang, X., Gu, Z., Fan, Q., Gibbons, W., Hoefelmeyer, J.D., Kharel, P.R., Shrestha, M., 2016: Hierarchical porous activated carbon for supercapacitor derived from corn stalk core by potassium hydroxide activation. Electrochimica Acta 212: 839-847.
2. Chandel, A.K., da Silva, S.S., Carvalho, W., Singh, O.V., 2012: Sugarcane bagasse and leaves: foreseeable biomass of biofuel and bio-products. Journal of chemical technology and biotechnology 87: 11-20.
3. Cheng, X.Y., Liu, C.Z., 2011: Hydrogen production via thermophilic fermentation of cornstalk by Clostridium thermocellum. Energy & Fuels 25: 1714-1720.
4. Corrales, R.C.N.R., Mendes, F.M.T., Perrone, C.C., Sant'Anna, C., de Souza, W., Abud, Y., da Silva Bon, E.P.P., Ferreira-Leitão, V., 2012: Structural evaluation of sugar cane bagasse steam pretreated in the presence of CO_2 and SO_2. Biotechnology for biofuels 5: 36.
5. Focher, B., Palma, M.T., Canetti, M., Torri, G., Cosentino, C., Gastaldi, G., 2001: Structural differences between non-wood plant celluloses: evidence from solid state NMR, vibrational spectroscopy and X-ray diffractometry. Industrial Crops and Products 13: 193-208.

6. Gao, Y., Xu, J., Zhang, Y., Yu, Q., Yuan, Z., Liu, Y., 2013: Effects of different pretreatment methods on chemical composition of sugarcane bagasse and enzymatic hydrolysis. Bioresource technology 144: 396-400.

7. Gigac, J., Fišerová, M., Stankovská, M., Pažitný, A., 2017: Enzymatic hydrolysis of extruded wheat straw with addition of sodium hydroxide and calcium hydroxide. Wood Research 62(6): 919-930.

8. Gramera, R.E., Whistler, R.L., 1963: Isolation of three polysaccharides from the hemicellulose B fraction of corn stalk. Archives of Biochemistry and Biophysics 101: 75-80.

9. Ioannidou, O., Zabaniotou, A., Antonakou, E.V., Papazisi, K.M., Lappas, A.A., Athanassiou, C., 2009: Investigating the potential for energy, fuel, materials and chemicals production from corn residues (cobs and stalks) by non-catalytic and catalytic pyrolysis in two reactor configurations. Renewable and sustainable energy reviews 13: 750-762.

10. Jarabo, R., Monte, M.C., Fuente, E., Santos, S.F., Negro, C., 2013: Corn stalk from agricultural residue used as reinforcement fiber in fiber-cement production. Industrial Crops and Products 43: 832-839.

11. Jiang, D., Ge, X., Zhang, T., Liu, H., Zhang, Q., 2016: Photo-fermentative hydrogen production from enzymatic hydrolysate of corn stalk pith with a photosynthetic consortium. International Journal of Hydrogen Energy 41: 16778-16785.

12. Kalderis, D., Bethanis, S., Paraskeva, P., Diamadopoulos, E., 2008: Production of activated carbon from bagasse and rice husk by a single-stage chemical activation method at low retention times. Bioresource technology 99: 6809-6816.

13. Kline, L.M., Hayes, D.G., Womac, A.R., Labbe, N., 2010: Simplified determination of lignin content in hard and soft woods via UV-spectrophotometric analysis of biomass dissolved in ionic liquids. BioResources 5: 1366-1383.

14. Li, P., Cai, D., Luo, Z., Qin, P., Chen, C., Wang, Y., Zhang, C., Wang, Z., Tan, T., 2016a: Effect of acid pretreatment on different parts of corn stalk for second generation ethanol production. Bioresource technology 206: 86-92.

15. Li, Y., Li, Y., Li, L., Shi, X., Wang, Z., 2016b: Preparation and analysis of activated carbon from sewage sludge and corn stalk. Advanced Powder Technology 27: 684-691.

16. Martın, C., Galbe, M., Wahlbom, C.F., Hahn-Hägerdal, B., Jönsson, L.J., 2002: Ethanol production from enzymatic hydrolysates of sugarcane bagasse using recombinant xylose-utilising *Saccharomyces cerevisiae*. Enzyme and Microbial Technology 31: 274-282.

17. Nanda, S., Mohanty, P., Pant, K.K., Naik, S., Kozinski, J.A., Dalai, A.K., 2013: Characterization of North American lignocellulosic biomass and biochars in terms of their candidacy for alternate renewable fuels. Bioenergy Research 6: 663-677.

18. Pang, C., Xie, T., Lin, L., Zhuang, J., Liu, Y., Shi, J., Yang, Q., 2012: Changes of the surface structure of corn stalk in the cooking process with active oxygen and MgO-based solid alkali as a pretreatment of its biomass conversion. Bioresource technology 103: 432-439.

19. Pažitný, A., Boháček, Š., Russ, A., 2011: Application of distillery refuse in papermaking: novel methods of treated distillery refuse spectral analysis. Wood Research 56(4): 533-544.

20. Pažitný, A., Russ, A., Boháček, Š., Bottová, V., Černá, K., 2013: Utilization of energetic grass fibre for modification of recovered fibre properties. Wood Research 58(2): 181-190.

21. Pažitný, A., Russ, A., Boháček, Š., Stankovská, M., Ihnát, V., Šutý, Š., 2019a: Various lignocellulosic raw materials pretreatment processes utilizable for increasing holocellulose accessibility for hydrolytic enzymes. Part II. Effect of steam explosion temperature on beech enzymatic hydrolysis. Wood Research 64(3): 437-448.

22. Pažitný, A., Russ, A., Boháček, Š., Stankovská, M., Šutý, Š., 2019b: Various lignocellulosic raw materials pretreatment processes utilizable for increasing holocellulose accessibility for hydrolytic enzymes. Part I. Evaluation of wheat straw pretreatment processes. Wood Research 64(1): 13-24.

23. Poletto, M., Dettenborn, J., Pistor, V., Zeni, M., Zattera, A.J., 2010: Materials produced from plant biomass: Part I: evaluation of thermal stability and pyrolysis of wood. Materials Research 13: 375-379.

24. Quan, C., Gao, N., Song, Q., 2016: Pyrolysis of biomass components in a TGA and a fixed-bed reactor: thermochemical behaviors, kinetics, and product characterization. Journal of Analytical and Applied Pyrolysis 121: 84-92.

25. Quesada, J., Rubio, M., Gómez, D., 1999: Ozonation of lignin rich solid fractions from corn stalks. Journal of wood chemistry and technology 19: 115-137.

26. Ragan, S., Megonnell, N., 2011: Activated carbon from renewable resources - Lignin. Cellulose Chemistry and Technology 45(7): 527-531.

27. Ren, N., Wang, A., Gao, L., Xin, L., Lee, D.J., Su, A., 2008: Bioaugmented hydrogen production from carboxymethyl cellulose and partially delignified corn stalks using isolated cultures. International journal of hydrogen energy 33: 5250-5255.

28. Scardi, P., Leoni, M., 2001: Diffraction line profiles from polydisperse crystalline systems. Acta Crystallographica Section A: Foundations of Crystallography 57: 604-613.

29. Singh, Y.D., Mahanta, P., Bora, U., 2017: Comprehensive characterization of lignocellulosic biomass through proximate, ultimate and compositional analysis for bioenergy production. Renewable energy 103: 490-500.

30. Song, C., Hu, H., Zhu, S., Wang, G., Chen, G., 2004: Nonisothermal catalytic liquefaction of corn stalk in subcritical and supercritical water. Energy & Fuels 18: 90-96.

31. Song, C.L., Zhang, Z.T., Chen, W.Y., Liu, C., 2009: Converting cornstalk into simple sugars with high-pressure nonequilibrium plasma. IEEE Transactions on Plasma Science 37: 1817-1824.

32. Song, W., Gao, B., Zhang, T., Xu, X., Huang, X., Yu, H., Yue, Q., 2015: High-capacity adsorption of dissolved hexavalent chromium using amine-functionalized magnetic corn stalk composites. Bioresource technology 190: 550-557.

33. Stankovská, M., Fišerová, M., Gigac, J., Pažitný, A., 2018: Effect of alkaline extrusion pretreatment of wheat straw on filtrate composition and enzymatic hydrolysis. Cellulose Chemistry and Technology 52(9-10): 815-822.

34. Sun, Y.G., Ma, Y., Wang, Z., Yao, J., 2014: Evaluating and optimizing pre-treatment technique for catalytic hydrogenolysis conversion of corn stalk into polyol. Bioresource technology 158: 307-312.

35. Sun, Y.G., Ma, Y.L., Wang, L.Q., Wang, F.Z., Wu, Q.Q., Pan, G.Y., 2015: Physico-chemical properties of corn stalk after treatment using steam explosion coupled with acid or alkali. Carbohydrate polymers 117: 486-493.

36. Uzun, B.B., Sarioğlu, N., 2009: Rapid and catalytic pyrolysis of corn stalks. Fuel Processing Technology 90: 705-716.

37. Wang, D., Sun, X.S., 2002: Low density particleboard from wheat straw and corn pith. Industrial Crops and Products 15: 43-50.

38. Wang, M., Leitch, M., Xu, C.C., 2009: Synthesis of phenolic resol resins using cornstalk-derived bio-oil produced by direct liquefaction in hot-compressed phenol–water. Journal of Industrial and Engineering Chemistry 15: 870-875.

39. Wang, Y.T., Chen, H., Wang, D.J., Bai, L.J., Xu, H., Wang, W.X., 2016: Preparation of corn stalk-based adsorbents and their specific application in metal ions adsorption. Chemical Papers 70: 1171-1184.

40. Xiao, B., Sun, X., Sun, R., 2001: Chemical, structural, and thermal characterizations of alkali-soluble lignins and hemicelluloses, and cellulose from maize stems, rye straw, and rice straw. Polymer degradation and stability 74: 307-319.

41. Xing, Y., Fan, S.Q., Zhang, J.N., Fan, Y.T., Hou, H.W., 2011: Enhanced bio-hydrogen production from corn stalk by anaerobic fermentation using response surface methodology. International Journal of Hydrogen Energy 36: 12770-12779.

42. Xu, F., Wang, D., 2015: Analysis of lignocellulosic biomass using infrared methodology. Pretreatment of Biomass 1: 7-25.

43. Xu, Z., Li, W., Du, Z., Wu, H., Jameel, H., Chang, H.M., Ma, L., 2015: Conversion of corn stalk into furfural using a novel heterogeneous strong acid catalyst in γ-valerolactone. Bioresource technology 198: 764-771.

44. Yan, L., Liu, N., Wang, Y., Machida, H., Qi, X., 2014: Production of 5-hydroxymethylfurfural from corn stalk catalyzed by corn stalk-derived carbonaceous solid acid catalyst. Bioresource technology 173: 462-466.

45. Yang, H., Yan, R., Chen, H., Lee, D.H., Zheng, C., 2007: Characteristics of hemicellulose, cellulose and lignin pyrolysis. Fuel 86: 1781-1788.

46. Yang, X., Zhang, S., Zuo, Z., Men, X., Tian, S., 2011: Ethanol production from the enzymatic hydrolysis of non-detoxified steam-exploded corn stalk. Bioresource technology 102: 7840-7844.

47. Ye, X.P., Liu, L., Hayes, D., Womac, A., Hong, K., Sokhansanj, S., 2008: Fast classification and compositional analysis of cornstover fractions using Fourier transform near-infrared techniques. Bioresource technology 99: 7323-7332.

48. Zabaniotou, A., Ioannidou, O., 2008: Evaluation of utilization of corn stalks for energy and carbon material production by using rapid pyrolysis at high temperature. Fuel 87: 834-843.

49. Zeng, Y., Zhao, S., Yang, S., Ding, S.Y., 2014: Lignin plays a negative role in the biochemical process for producing lignocellulosic biofuels. Current opinion in biotechnology 27: 38-45.

50. Zhang, T., Li, W., Xu, Z., Liu, Q., Ma, Q., Jameel, H., Chang, H.M., Ma, L., 2016: Catalytic conversion of xylose and corn stalk into furfural over carbon solid acid catalyst in γ-valerolactone. Bioresource technology 209: 108-114.

51. Zhao, X., Chen, J., Chen, F., Wang, X., Zhu, Q., Ao, Q., 2013: Surface characterization of corn stalk superfine powder studied by FTIR and XRD. Colloids and Surfaces B: Biointerfaces 104: 207-212.

Thulani Shabangu, Linda Z. Linganiso, Tshwafo E. Motaung*
University of Unizulu Kwadlangezwa
Department of Chemistry
Kwadlangezwa Campus
Private Bag X1001, 3886
South Africa
*Corresponding author: motaungt@unizulu.ac.za

Motloung V. Setumo
Nelson Mandela University
Department of Physics
P.O. Box 77000
Port Elizabeth 6031
South Africa

Lehlohonolo F. Koao
University of The Free State
Department of Physics
Qwaqwa Campus
Private Bag X13
Phuthaditjhaba 9866
South Africa